Chemical Engineering Journal 143 (2008) 161–166

Contents lists available at ScienceDirect

Chemical Engineering Journal

journal homepage: www.elsevier.com/locate/cej

Investigation of reduction kinetics of $Cr_2O_7^{2-}$ in $FeSO_4$ solution

Fatih Sevim*, Derya Demir

Department of Chemical Engineering, Engineering Faculty, Atatürk University, 25240 Erzurum, Turkey

ARTICLE INFO

Article history:
Received 9 April 2007
Received in revised form 13 March 2008
Accepted 18 March 2008

Keywords:
Chrome
Electrochemistry
Reduction kinetics
Chemical reaction control model

ABSTRACT

The kinetics of reduction of potassium dichromate ($K_2Cr_2O_7$) by Fe^{2+} ions in sulfuric acid (H_2SO_4) solution have been investigated under well-defined hydrodynamic conditions. The reaction has been monitored potentiometrically by measuring volt values between saturated calomel electrode and a Pt electrode. The effect of stirring rate, particle size, temperature, Fe^{2+} and H^+ concentrations have been studied. It was found that the reaction kinetic model achieved in the study was chemical reaction control model. The reaction has been analyzed using kinetic equation $t = \tau(1-(1-x)^{1/3})$. The rate has been found proportional to $[Fe^{2+}]^{0.5}[H^+]^{0.5}$ and the apparent activation energy has been determined as 46.18 kJ mol^{-1}.

1. Introduction

Chromium is widely used in various industrial applications. If chromium polluted waters are discharged into the environment without any treatment, chromium content of surface and groundwater and soil considerably increases [1,2]. Chromium appears to be a nutrient for at least some plants and animals, including humans, although chromium(VI) species have been reported to be toxic to bacteria, plants, and animals. Chromium(III) is generally absorbed through cell membranes albeit to a significantly lesser degree than chromium(VI). Because Cr(VI) is more toxic than Cr(III), Cr(VI) analyzed in environmental samples is more important and has been accepted as more problematic chromium form in comparison to Cr(III). Although Cr(VI) is a strong oxidant, Cr(III) does not have not an oxidation property. Second important difference is that Cr(III) ions may cross easily and speedily from cell diaphragm than Cr (IV) [3].

The permissible limit of Cr(VI) in potable water is 0.05 mg l^{-1}, but for industrial and mining effluents the discharge value is around 0.5 mg l^{-1}. Since most of the industrial and mine effluents contain higher than the permissible limit, treatment to reduce/remove the pollutant before discharge into the environment becomes inevitable [4].

There are numerous works in literature dealing with the removal of chromium. In one of the works, a new possibility to selectively remove neutral salts contained in spent chromium tanning solutions has been presented with a view to achieving more efficient recycling of unused chromium as well as water. The membrane separation procedure described here offers a new possibility to reuse water, neutral salts and chrome without any attendant problems in process control or effluent treatment [5].

Greju and Lovi [6] studied the kinetics of Cr(VI) reduction by scrap iron in batch system, for aqueous solutions having low buffering capacities, as a function of pH (2.10–7.10), temperature (10–40 °C) and Cr(VI) concentration (19.2–576.9 μM). They reported that a kinetic expression was developed to describe reduction of chromium by scrap iron over the pH range of 4.17–7.10 and Cr(VI) concentration range of 19.2–38.4 μM [6].

The batch removal of hexavalent chromium (Cr(VI)) from wastewater under different experimental conditions using various adsorbents has been investigated [7].

According to the work of Hossain [8], the reaction rate expression for Cr(VI) reduction is nonlinear and the rate constants are evaluated by employing nonlinear optimization techniques. The outcome of the optimization techniques, in general, depends on the initial estimate of the kinetic parameters which is not always available. A graphical approach based on sound mathematical reasoning has been developed which is accurate, simpler to use, and can provide the best initial estimate for nonlinear optimization [8].

During the electrochemical reduction period of porous titanium dioxide in the calcium chloride solution, consecutive reactions have been observed Alexander et al. [9]. Under well-defined hydrodynamic conditions, reduction kinetics of MnO_2 by Fe^{2+} has been investigated [10].

The aim of this study is to explore the kinetics of Cr(VI) reduction by Fe^{2+} ions in sulfuric acid (H_2SO_4) solution under well-defined hydrodynamic conditions. The effect of stirring rate, particle size, temperature, Fe^{2+} and H^+ concentrations have been studied. It was

* Corresponding author. Tel.: +90 4422314555; fax: +90 4422360957.
E-mail address: fsevim@atauni.edu.tr (F. Sevim).

1385-8947/$ – see front matter © 2008 Elsevier B.V. All rights reserved.
doi:10.1016/j.cej.2008.03.013

Nomenclature

b	stoichiometric coefficient
C_A	$FeSO_4$ concentration
C_B	H_2SO_4 concentration
e	electrode potential
E_a	activation energy (kJ mol^{-1})
E	emf between Pt and saturated calomel electrode (V)
F	Faraday constant
k	reaction rate constant (s^{-1})
k_s	rate constant for surface reaction (cm s^{-1})
k_0	Frequency or pre-exponential factor (s^{-1})
m_0	amount of $K_2Cr_2O_7$ charged in the reactor (g)
R	universal gas constant (kJ mol^{-1} K^{-1})
R_s	0.4275×10^{-3} m (average radius of solid particles)
t	reaction time (s)
T	temperature (K)
V	reaction volume (m^3)
x	$K_2Cr_2O_7$ conversion

Greek letters

ρ_B	9.102×10^4 mol m^{-3} ($K_2Cr_2O_7$'s molar density)
τ	time required for complete conversion (s)

found that the reaction kinetic model obtained in this study was chemical reaction control model.

2. Experimental

Experiments were conducted in a 0.75 l jacketed cylindrical glass reactor of 0.1 m diameter. It was equipped with four baffles equally spaced. The flanged cover of the reactor contained sockets for a stirrer, a thermometer, a reflux condenser, inert gas entrance, a Pt electrode and a salt bridge. The stirring rate was controlled to ± 1 min^{-1} and temperature of the reactor was maintained within ± 0.1 °C. Helium gas was passed through the reactor to prevent oxidation of Fe^{2+} by air.

All aqueous solutions were prepared with pure water. The chemicals used were as received without further purification: potassium dichromate ($K_2Cr_2O_7$), H_2SO_4, Ferro(II) sulfate ($FeSO_4{\cdot}7H_2O$), potassium chloride (KCl) (Merck, Germany) was prepared according to the method described in Furmann [11]. In addition, the samples were sieved using ASTM standard sieves, giving particle size fractions of 0.550, 0.427, 0.303, 0.215 mm. The volume of $FeSO_4$ and H_2SO_4 solutions (constant 500 ml) was charged in the reactor, while the amount of $K_2Cr_2O_7$ used in the experiments was in the range of 0.2–0.35 g.

The maximum concentration change in all experiments was limited to 5%. Temperature and reactant concentrations were carefully selected so that no $Fe(OH)_3$ precipitate and higher conversion was detected at the end of experiments. The experimental facility for Cr^{4+} removal process is schematically shown in Fig. 1.

The most important property of this process is to evaluate the acid pickling solution which is being the waste product of steel industry. Acid pickling solution includes H_2SO_4 0.5–10% and $FeSO_4$ 10–12%.

The reaction of $K_2Cr_2O_7$ with Fe^{2+} ions in an acidic medium is governed by the equation:

$$Cr_2O_7^{2-} + 14H^+ + 6e^- \rightarrow 2Cr^{3+} + 7H_2O \quad E_0 = 1.33\,V \tag{1}$$

$$6Fe^{2+} \rightarrow 6Fe^{3+} + 6e^- \quad E_0 = -0.771\,V \tag{2}$$

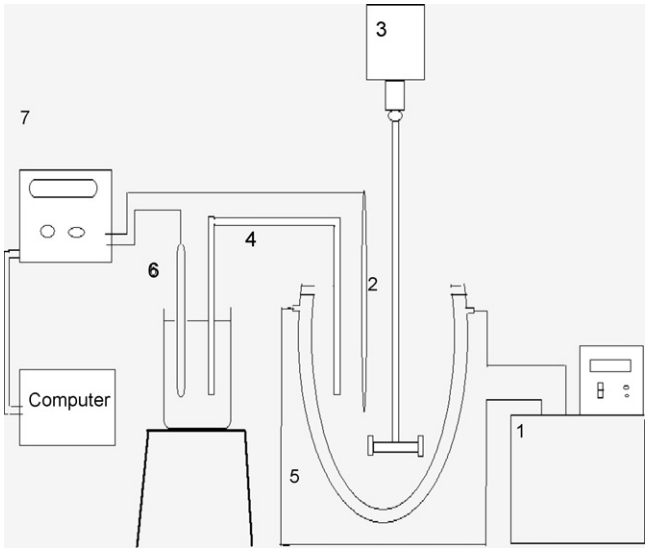

Fig. 1. Schematic diagram of the experimental setup: (1) water cooled bath; (2) Pt electrode; (3) mechanical stirrer; (4) salt bridge; (5) reactor; (6) calomel electrode; (7) multimeter.

$$Cr_2O_7^{2-} + 6Fe^{2+} + 14H^+ \rightarrow 2Cr^{3+} + 7H_2O + 6Fe^{3+} \quad E = 0.559\,V \tag{3}$$

The reaction was monitored by measuring the electromotive force (emf) between a saturated calomel electrode and a Pt electrode. For this purpose a voltmeter, with 0.5 mV precision, connected to a computer was used.

According to above reaction, volt change obtained with oxidation of Fe^{2+} ions into Fe^{3+} ions was graphed versus time by computing the values obtained from multimeter. The conversion values were computed using the recorded millivolt values and these estimates were introduced into kinetic equations.

The reaction conversions from voltage measurements were calculated as follows:

The emf of the cell is:

$$E = e^0 - \frac{RT}{F} \ln\left[\frac{a_{Fe^{2+}}}{a_{Fe^{3+}}}\right] = [e_{Fe^{2+}/Fe^{3+}} - e_{cal}] - \frac{RT}{F} \ln\left[\frac{a_{Fe^{2+}}}{a_{Fe^{3+}}}\right] \tag{4}$$

The calomel electrode (e_{cal}) was used as an anode. According to given as $e^0 = 0.2415$ V standard electromotive force for saturated calomel electrode, $e^0 = 0.77$ V standard electromotor force for Fe^{2+} and Fe^{3+} redox double:

$$E = 0.5285 + \frac{RT}{F} \ln\left[\frac{a_{Fe^{3+}}}{a_{Fe^{2+}}}\right] \tag{5}$$

As the composition of the solution changes very little during reaction, the ionic strength and the activity coefficients remain almost constant. It is shown as E_0 electromotive force in initial, E_1 for $x = 1$ and E_x for any x conversion, and thus Eq. (5) may be written as:

$$E_0 = A + \frac{RT}{F} \ln\frac{[Fe_0{}^{3+}]}{[Fe_0{}^{2+}]} \tag{6}$$

$$E_x = A + \frac{RT}{F} \ln\frac{[Fe_x{}^{3+}]}{[Fe_x{}^{2+}]} \tag{7}$$

$$E_1 = A + \frac{RT}{F} \ln\frac{[Fe_1{}^{3+}]}{[Fe_1{}^{2+}]} \tag{8}$$

The initial concentration ratio, $[Fe_0^{3+}]/[Fe_0^{2+}]$, was approximately equal to 10^{-3} in each experiment, so E_0 values were in the same order magnitude.

During experiment, $[Fe_x^{2+}] = [Fe_0^{2+}]$ may be accepted, since Fe^{2+} changes maximum to 5%. When Eqs. (6) and (7), (6) and (8) extracted side by side using this acceptance

$$E_x - E_0 = \frac{RT}{F} \ln \left[\frac{[Fe_x^{3+}]}{[Fe_0^{3+}]} \right] \quad (9)$$

$$E_1 - E_0 = \frac{RT}{F} \ln \left[\frac{[Fe_1^{3+}]}{[Fe_0^{3+}]} \right] \quad (10)$$

Eqs. (9) and (10) are obtained. These equations are rearranged:

$$[Fe_x^{3+}] = [Fe_0^{3+}] \exp \frac{E_x - E_0}{RT/F} \quad (11)$$

$$[Fe_1^{3+}] = [Fe_0^{3+}] \exp \frac{E_1 - E_0}{RT/F} \quad (12)$$

Stoichiometry of reaction (3) into consideration, following equality between concentration of Fe^{3+} and the mass of $K_2Cr_2O_7$ has been obtained ($m_0 = K_2Cr_2O_7$ amount (g), $V = Fe^{3+}$ volume of solution (l), $x = K_2Cr_2O_7$ conversion).

$$\frac{m_0 x}{294V} = [Fe_x^{3+}] - [Fe_0^{3+}] \quad (13)$$

And, for $x = 1$:

$$\frac{m_0}{294V} = [Fe_1^{3+}] - [Fe_0^{3+}] \quad (14)$$

The expressions are obtained. If Eqs. (13) and (14) are compared each other:

$$x = \frac{[Fe_x^{3+}] - [Fe_0^{3+}]}{[Fe_1^{3+}] - [Fe_0^{3+}]} \quad (15)$$

Finally, from Eqs. (11), (12) and (15)

$$x = \frac{\exp[(E_x - E_0)/(RT/F)] - 1}{\exp[(E_1 - E_0)/(RT/F)] - 1} \quad (16)$$

Using Eq. (16), volt values have been transformed to transformation values.

3. Results and discussions

3.1. Kinetic analysis

Fluid–solid heterogeneous reaction systems have many applications in chemical and hydrometallurgical processes. A successful reactor design for these processes depends strongly on kinetic data. In such systems, the reaction rate can be generally controlled by one of the following steps: diffusion through the fluid film, diffusion through the ash, or chemical reaction at the surface of the core of unreacted materials [12]. In order to obtain the conversion values from the experimentally calculated volt values Eq. (16) was used. From the results of the statistical analyses, it was found that the kinetics of reduction of $Cr_2O_7^{2-}$ by Fe^{2+} ions in H_2SO_4 solution is controlled by chemical reaction.

Also, it was determined that the integral rate expression obeyed the equation:

$$\frac{t}{\tau} = 1 - (1 - x)^{1/3} \quad (17)$$

$$\tau = \frac{\rho_B R_s}{b k_s C_A} \quad (18)$$

Since the reaction has ended in a very short time for the high concentrations at pre-experiments, $FeSO_4$ and H_2SO_4 concentrations were adjusted to be in low concentrations in order to avoid the experimental error. Temperature range was chosen between 10 and 65 °C because of the sensitivity of the employed calomel electrode.

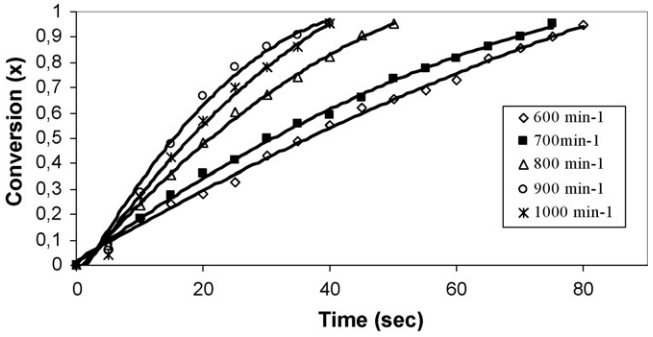

Fig. 2. Effect of stirring rate on conversion, at 20 °C, particle size 0.427 mm, 0.2 M $FeSO_4$, 0.03 M H_2SO_4.

3.2. The effect of stirring rate

It is well known that a minimum stirring rate is required for complete suspension of particles in a liquid medium and that, below this critical speed, the total surface area of particles is not available for reaction and also the rate of mass transfer depends strongly on stirring rate. Rate experiments which aim to discriminate between a diffusion controlled rate model and a chemically controlled one have to be conducted at stirring speeds above this critical value. Thus, it is very important to know the value of the critical rate. Experiments at 600, 700, 800, 900 and 1000 min^{-1} were carried out. The results are shown in Fig. 2. An increase in low stirring speeds increased the dissolution rate because a complete suspension could not be provided (Fig. 2). But, in high stirring speeds, it was observed that the stirring speed had not a significant effect on the dissolution rate. Above 900 min^{-1} reaction rate was not influenced by stirring rate so diffusion effects across the liquid film around $K_2Cr_2O_7$ particles seemed to be negligible.

3.3. The effect of particle size

The effect of four different particle sizes: 0.550, 0.427, 0.303 and 0.215 mm were investigated. From Fig. 3, it can be seen that the reaction rate is inversely proportional to particle size. The results show that the particle size has a significant effect on the dissolution rate of chromate. It is seen that the percentage dissolution of chromate increases with time and decreases with particle size. This

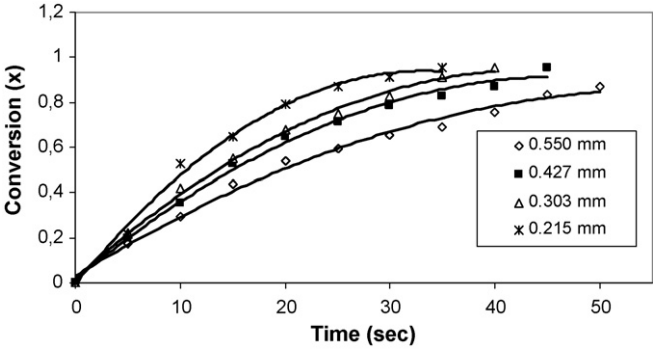

Fig. 3. Effect of particle size on conversion, at 20 °C, 900 min^{-1} stirring rate, 0.2 M $FeSO_4$, 0.03 M H_2SO_4.

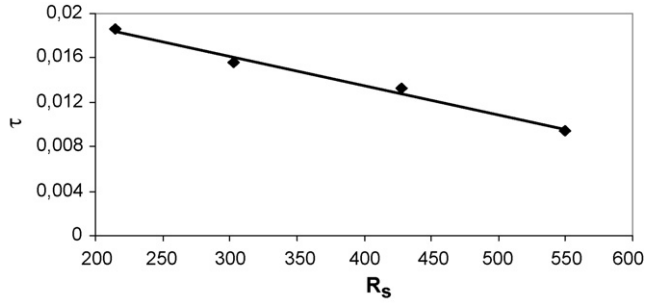

Fig. 4. Plot of τ vs. R_s.

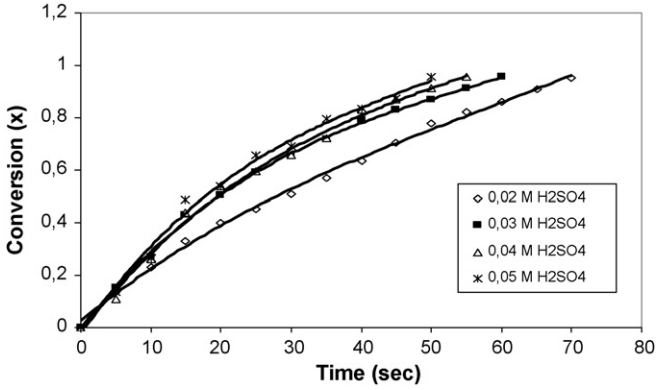

Fig. 5. Effect of different H_2SO_4 concentration on conversion, at 20 °C, 900 min^{-1} stirring rate, 0.427 mm particle size, 0.2 M $FeSO_4$.

situation is attributed to an increase in surface area per unit weight as the particle size decreases.

When the reaction is chemically controlled, particle size and τ values should be changed linearly (Eq. (18)). If the τ values are plotted versus particle size, obtained curve is straight line and this verifies that the reaction is chemically controlled (Fig. 4)

3.4. The effect of concentrations

The effects of various H_2SO_4 and $FeSO_4$ concentrations (C_B and C_A, respectively) were investigated. Chosen concentrations for H_2SO_4 were 0.02, 0.03, 0.04 and 0.05 M and for $FeSO_4$ were 0.1, 0.15, 0.2 and 0.25 M (Figs. 5 and 6).

$1-(1-x)^{1/3}$ versus time has been plotted for various $FeSO_4$ concentrations and τ values were estimated considering the slope of these plots (Fig. 7).

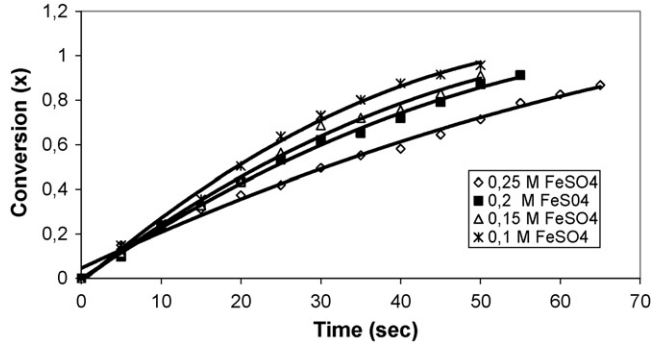

Fig. 6. Effect of different $FeSO_4$ concentration on conversion, at 20 °C, 900 min^{-1} stirring rate, 0.427 mm particle size, 0.03 M H_2SO_4.

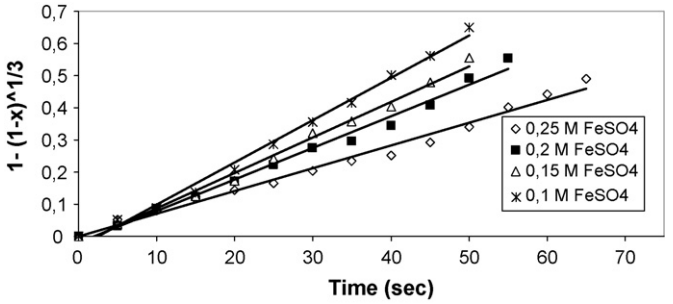

Fig. 7. Plot of $1-(1-x)^{1/3}$ vs. time for concentration 0.03 M H_2SO_4 and different $FeSO_4$ concentrations.

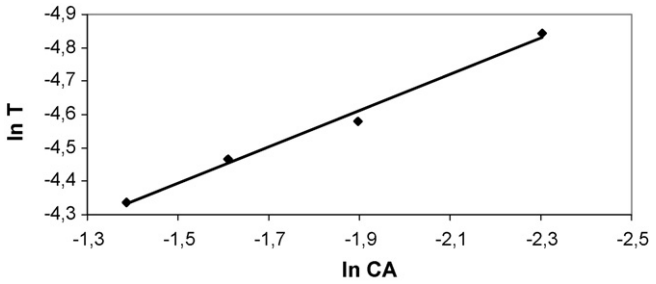

Fig. 8. Plot of $\ln C_A$ vs. $\ln \tau$.

Concentration relation for τ values is given in Eq. (19),

$$f(C_{Fe^{2+}}, C_{H^+}) = C^a_{Fe^{2+}} C^b_{H^+} \quad (19)$$

Eq. (19) can be arranged as follows

$$\tau = \frac{\rho_B R_s}{k C^a_{Fe^{2+}} C^b_{H^+}} \quad (20)$$

$$\frac{\rho_B R_s}{k C^b_{H^+}} = \alpha \quad (21)$$

When Eq. (21) is introduced in Eq. (20) and taking the logarithm of Eq. (20), Eq. (22) can be obtained.

$$\ln \tau = \ln \alpha - a \ln C_{Fe^{2+}} \quad (22)$$

In order to estimate the value of a, $\ln C_A$ versus $\ln \tau$ should be plotted and the slope of the straight line should be computed. Obtained a value is 0.544–0.5 (Fig. 8).

$1-(1-x)^{1/3}$ versus time has been plotted for different acid concentrations (H_2SO_4) and τ values were estimated considering the slope of these plots (Fig. 9). In order to estimate the b value, $\ln C_B$ versus $\ln \tau$ should be plotted and the slope of the straight line should

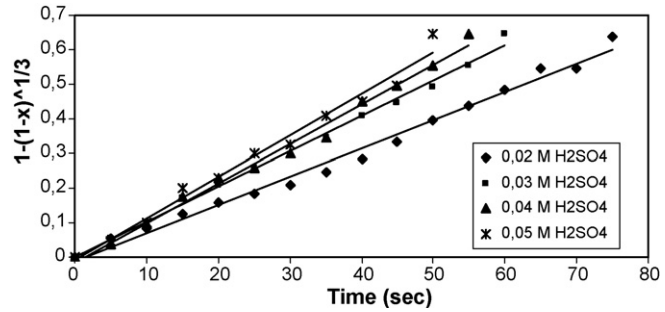

Fig. 9. Plot of $1-(1-x)^{1/3}$ vs. time for concentration 0.2 M $FeSO_4$ and different H_2SO_4 concentrations.

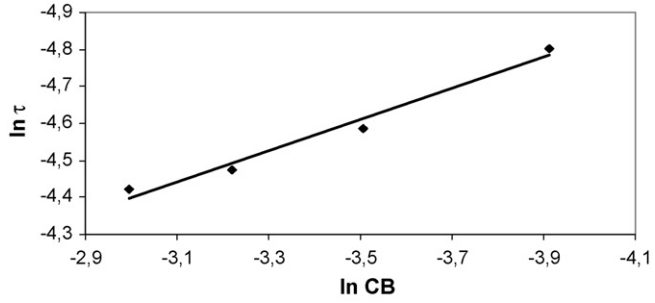

Fig. 10. Plot of $\ln C_B$ vs. $\ln \tau$.

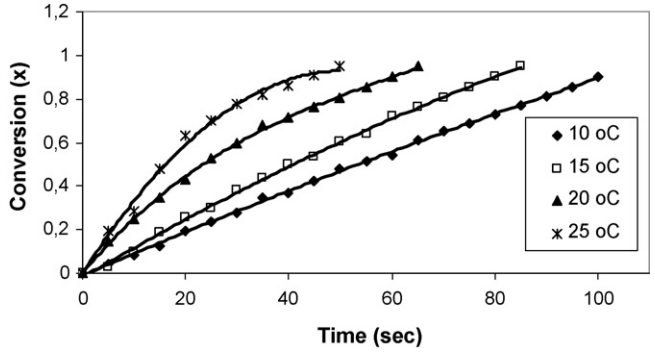

Fig. 11. Effect of temperature on conversion, at 900 min^{-1} stirring rate, 0.427 mm particle size, 0.03 M H_2SO_4 and 0.2 M $FeSO_4$.

be computed under the conditions where C_A is constant and C_B is variable (Fig. 10). Computed b value is 0.421–0.5.

3.5. The effect of reaction temperature

Investigated temperatures were 10, 15, 20 and 25 °C (Fig. 11). $1-(1-x)^{1/3}$ versus time has been plotted for different temperature and τ values were estimated considering the slope of these plots (Fig. 12). In order to estimate the τ values from Eq. (20) k values were found at different temperatures. $1/T$ versus $\ln k$ was plotted and the apparent activation energy (E_a) was computed from the slope of the straight line (Fig. 13).

$$k = k_0\, e^{-E_a/RT} \tag{23}$$

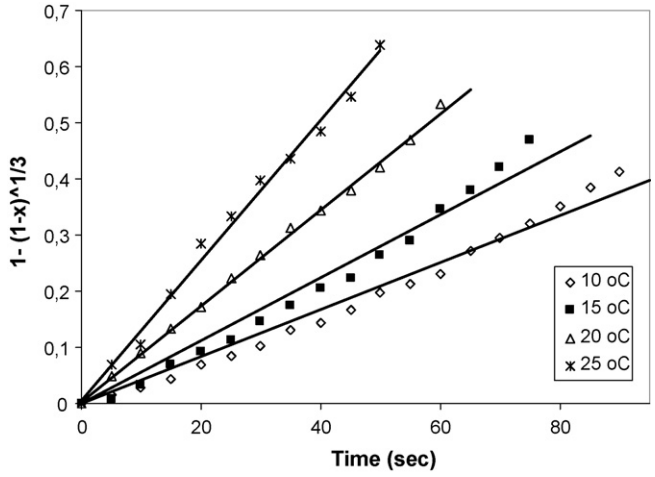

Fig. 12. Plot of $1-(1-x)^{1/3}$ vs. time at various temperatures.

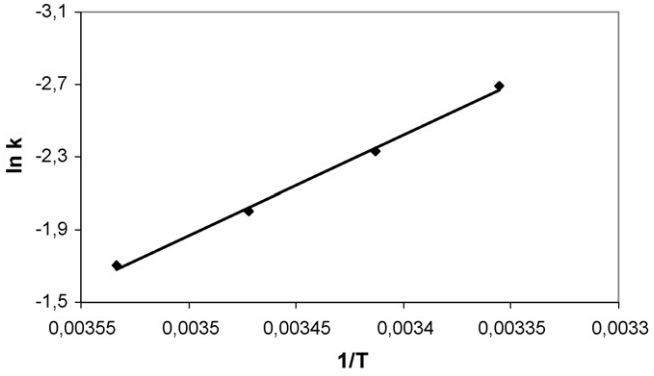

Fig. 13. Arrhenius plot of $\ln k$ vs. $1/T$.

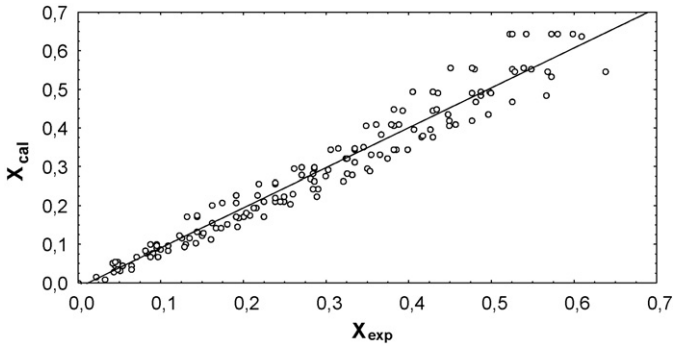

Fig. 14. Agreement between experimental and calculated conversion values.

$$\ln k = \ln K_0 - \frac{E_a}{RT} \tag{24}$$

Found values for E_a and k_0 are 46.184 kJ mol^{-1} and 5.54×10^{10}, respectively.

4. Conclusions

Since most of the industrial and mine effluents contain higher chromate than the permissible limit, treatment to reduce/remove the pollutant before discharge into the environment becomes inevitable.

Considering the all related parameters, a general equation shown in below was developed for the reduction kinetics of $Cr_2O_7^{2-}$;

$$[1-(1-x)^{1/3}] = \frac{5.54 \times 10^{10}[Fe^{2+}]^{0.5}[H^+]^{0.5}(e^{-(46,184/RT)})}{\rho_B R_s}\, t \tag{25}$$

The effect of stirring speed was investigated in the range 600–1000 min^{-1}. The conversion values increase with increasing stirring speed.

Conversion of reaction was independent of stirring speeds from 900 min^{-1} and higher. Thus, 900 min^{-1} was adopted. Decreasing particle size led greater surface area. Hence, conversion rates raised proportionally because of increased surface area between reactant and solid particle. Investigated temperatures were 10, 15, 20 and 25 °C for conversion rates. It was also found that increasing temperature increased the conversion rate. The effect of H_2SO_4 concentration on conversion rates was studied and found that increasing acid concentration increased the conversion rate.

As seen in Eq. (20), Figs. 8 and 10, since τ and R_s are linear curves and the upper values of concentration are 1 in total, it indicates that reaction is chemically controlled according to "Shrinking Core Model" [12].

To test the agreement between the experimental conversion and the values calculated from the semi empirical model, the graph of x_{exp} versus x_{cal} was plotted as shown in Fig. 14. It is observed that the agreement between the experimental and calculated values is very good with a correlation coefficient of 0.970 and standard deviation of ±0.00644 [13].

Acknowledgement

This research was financially supported by the Atatürk University Research Council (Project No.: 2002/35).

References

[1] J. Kotas, Z. Stasicka, Chromium occurrence in the environment and methods of its speciation, Environ. Pollut. 107 (3) (2000) 263–283.
[2] M. Pantsar-Kallio, S.-P. Reinikainen, M. Oksanen, Interactions of soil components and their effects on speciation of chromium in soils, Anal. Chim. Acta 439 (2001) 9–17.
[3] D.E. Kimbrough, Y.E. Cohen, A.M. Winer, L.M. Creelman, C.M. Mabuni, A Critical assessment of chromium in the environment, Crit. Rev. Environ. Sci. Technol. 29 (1) (1999) 1–46.
[4] K. Selvaraj, S. Manonmani, S. Pattabhi, Removal of hexavalent chromium using distillery sludge, Bioresour. Technol. 89 (2003) 207–211.
[5] J. Raghava Rao, B.G.S. Prasad, V. Narasimhan, T. Ramasami, P.R. Shah, A.A. Khan, Electrodialysis in the recovery and reuse of chromium from industrial effluents, J. Membr. Sci. 46 (2–3) (1989) 215–224.
[6] M. Greju, A. Lovi, Kinetics of hexavalent chromium reduction by scrap iron, J. Hazad. Mater. B 135 (2006) 66–73.
[7] N.K. Hamadi, X.D. Chen, M.M. Farid, M.G.Q. Lu, Adsorption kinetics for the removal of chromium(VI) from aqueous solution by adsorbents derived from used tyres and sawdust, Chem. Eng. J. 84 (2001) (2001) 95–105.
[8] M.D. Hossain, Graphical estimation of the dual-enzyme kinetic parameters for Cr(VI) reduction, Chemosphere 63 (2005) 171–174.
[9] D.T.L. Alexander, C. Schwandt, D.J. Fray, Microstructural kinetics of phase transformations during electrochemical reduction of titanium dioxide in molten calcium chloride, Acta Materialia 54 (2006) 2933–2944.
[10] M. Bayramoğlu, T. Tekin, An electrochemical model for reduction of MnO_2 with Fe^{2+} ions, J. Appl. Electrochem. 23 (1993) 1273–1279.
[11] N.H. Furmann, Standard Methods of Chemical Analysis, 6th ed., Van Nostrand Reinhold, New York, 1963.
[12] O. Levenspiel, Chemical Reaction Engineering, John Wiley & Sons, New York, 1999.
[13] Z.I. Zafar, M. Ashraf, Selective leaching kinetics of calcareous phosphate rock in lactic acid, Chem. Eng. J. 131 (2007) 41–48.